Neutron Reflectivity and Computer Simulation Studies of Self-Assembled Brushes Formed by Centrally Adsorbed Star Polymers

ARTICLE *in* MACROMOLECULES · JANUARY 2008

Impact Factor: 5.8

1 AUTHOR:

Georgios Sakellariou

National and Kapodistrian University of At…

58 PUBLICATIONS **603** CITATIONS

SEE PROFILE

Neutron Reflectivity and Computer Simulation Studies of Self-Assembled Brushes Formed by Centrally Adsorbed Star Polymers

Ioannis Hiotelis,[†] Alexandros G. Koutsioubas,[†] Nikolaos Spiliopoulos,[†] Dimitris L. Anastassopoulos,[†] Alexandros A. Vradis,[†] Chris Toprakcioglu,*[,†] Alain Menelle,[‡] George Sakellariou,[§] and Nikos Hadjichristidis[§]

Physics Department, University of Patras, Patras 26500, Greece 26500; Laboratoire Leon Brillouin, CEA SACLAY, 91191 Gif-sur-Yvette Cedex, France; and Chemistry Department, University of Athens, Panepistimioupoli Zografou 15771, Greece

Received December 10, 2007; Revised Manuscript Received June 25, 2008

ABSTRACT: The equilibrium properties of polymer brushes formed by starlike polymers with varying number of arms attached to a surface by their center were studied experimentally with neutron reflectrometry (NR). Polystyrene (PS) stars in a good solvent (toluene) were centrally adsorbed onto a quartz substrate via a zwitterionic anchor group. Increasing the number of arms resulted in significantly lower equilibrium adsorbance, while replacement experiments of a 3-armed star brush by linear chains revealed interesting equilibrium and kinetic features related to the special architecture of star polymers. These results are compared with scaling theoretical calculations and Monte Carlo simulations of centrally adsorbed star polymers that were performed under the bond fluctuation simulation scheme. Several features of the experimental results are reproduced in our simulation study.

Introduction

Flexible polymer chains end-tethered to a surface in good solvent tend to extend away from the surface due to excluded volume interactions. At sufficiently high grafting densities the chains become elongated normal to the surface, this extension being opposed by an elastic restoring force of entropic origin to form a layer of stretched chains, referred to as a "polymer brush". These systems have been studied extensively in recent years by numerous experimental techniques, simulation, and theoretical methods.[1−7]

Polymer brushes can be grown chemically from a surface or can be formed by block copolymer self-assembly procedures where one block dissolves in the solvent and the other block adsorbs on a surface. Self-assembled brushes of end-functionalized polystyrene (PS) with a short anchor block have been prepared in the case where the anchor block is either a small polymer chain such as poly(ethylene oxide) (PEO)[8] or a small molecule such as a sulfozwitterionic end group.[9]

For such systems, the variation of the brush height is dependent on the copolymer molecular weight and sticking energy of the anchor block. The variation of the brush height with molecular weight has been experimentally investigated in earlier works.[8,10,11] In particular, the results of Taunton et al.[10] have been found to agree well with the prediction of scaling theory.[5,6,10]

Our purpose here is to extend the studies of polymer brushes by varying the number of chains attached to a surface by a single anchor block of constant sticking energy. Instead of increasing the molecular weight of a macromolecule by increasing its chain length, we accomplish this by linking shorter chains through their ends to a common central point. We use polystyrene chains (fPS$_{70K}$)-X with $f = 1$, 2, and 3 functionalized at one end by a zwitterionic group X = $(CH_3)_2N^+(CH_2)_3SO_3^-$ attached via short (molecular weight ca. 500) polybutadiene spacers in order to study the effect of multiple arms on the brush equilibrium properties. In an earlier investigation Dhoot et al.[12] explored the idea of tethering more than one chain via a common anchoring block by using linear PS−PVP−PS triblocks, where the PVP block acts as an anchor. In the present study, however, our centrally tethered star polymers have their center adsorbed on a plane surface via a single zwitterion and present topological differences from free star polymers in solution or grafted linear polymers.

The adsorption behavior of end-functionalized star polymers has been experimentally studied previously.[13] Star polymers that are terminally attached by one of their arms have also been considered in theoretical[14,15] and simulation works.[16,17] The present investigation is the first detailed experimental work on the adsorption of center-functionalized starlike polymers at solid−liquid interfaces that result in brush formation. Here, using neutron reflectivity techniques, we study the adsorbed amount, brush height, surface density, and volume fraction profile of these copolymer layers as the number of chain arms increases.

Star polymers have received much attention in recent years due to their unique properties, since they represent a class of macromolecules with intermediate characteristics between colloids and polymers.[18,19] The prediction and interpretation of conformational properties of starlike polymers in solution or near a surface are more difficult in comparison to linear chains due to the complexity of these structures and the fact that all the branches have to join at the center. This geometric constraint leads to different concentration regimes at the core and at the outside region of the star structure. A scaling theory has been proposed[20] concerning free stars in solution while theoretical[21,22] and computer simulation work[23] has been carried out for the determination of various configurational and statistical properties of center-adsorbed topologies.

Since there is no detailed theoretical approach of polymer brushes formed by star-shaped polymers, we compare the main features of the current experimental results with scaling arguments and simulation data from bond fluctuation Monte Carlo (BFMC) simulations of center adsorbed star polymers. Additionally, the potential replacement of a brush layer of centrally adsorbed star polymers by the introduction of another linear polymer in solution is studied. The experimental results and

* Corresponding author. E-mail: ctop@physics.upatras.gr.
[†] University of Patras.
[‡] CEA SACLAY.
[§] University of Athens.

10.1021/ma702749z CCC: $40.75
Published on Web 09/24/2008

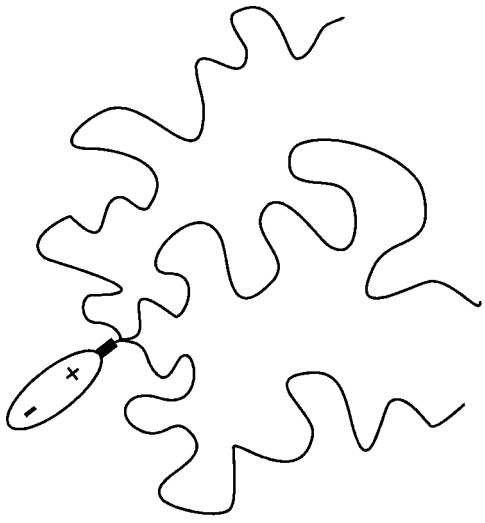

Figure 1. Schematic representation of a center-functionalized three-armed star. The centrally located zwitterion is used to anchor the star onto quartz substrates.

Table 1. Molecular Characteristics of Star Polymers Used in This Study

sample	M_w	M_w/M_n
PS_{70K}-X	78 000	1.07
$2PS_{70K}$-X	156 000	1.04
$3PS_{70K}$-X	234 000	1.03

their comparison with scaling theory and simulation data are of interest especially in relation to applications such as colloidal stabilization, separation of colloidal mixtures, lubrication, and adhesion.

Experimental Section

a. Materials. Three ($f$$PS_{70K}$)-X, one linear and two miktoarm star end-functionalized copolymers, where the zwitterionic group X is $(CH_3)_2N^+(CH_2)_3SO_3^-$, were used in this study. These macromolecules were synthesized by high-vacuum anionic polymerization techniques.[9] The linear diblock copolymer consisted of a dimethylamino end-functionalized short polybutadiene (PB) block (M_n = 500) and a polystyrene second block (M_n = 70 000). The three and four miktoarm star copolymers consisted of one short polybutadiene arm (M_n = 500) synthesized using [3-(dimethylamino)propyl]lithium as initiator. The PB block was connected by linking chemistry to two and three polystyrene chains having M_n = 70 000 each (see Figure 1). The amine polymers were converted to the sulfozwitterionic ones by reaction of the dimethylamino groups with excess of cyclopropanosultone. Characterization of these macromolecules is given in Table 1.

b. Neutron Reflectivity. Neutron reflectivity measurements were carried out at the Laboratoire Leon Brillouin in Saclay using the EROS time-of-flight spectrometer.[24] The angle of incidence, θ, was 0.75°, and the wavelength was in the range of 2−30 Å. The reflectivity was measured as a function of the scattering vector **Q**, where $|\mathbf{Q}| = Q = (4\pi/\lambda) \sin \theta$. It is well-known that neutron reflectometry is a very sensitive technique, which can provide valuable information on the volume fraction profile of adsorbed polymers normal to the reflecting interface.[25−27]

Adsorption was studied on optically flat quartz slabs. Before measurements the quartz substrates were cleaned in 3:1 (v/v) H_2SO_4−HNO_3 followed by 3:1 (v/v) HCl−HNO_3 for 6 h each. Then, substrates were washed in distilled water followed by a rinse with absolute ethanol. Reflectivity measurements were taken with the aid of a Teflon cell containing the polymer solution and the optically flat quartz slab as substrate.[8] Solutions of the copolymers in d-toluene (a good solvent for PS) at a concentration of 0.1 mg/mL were used for adsorption. From previous studies it is known

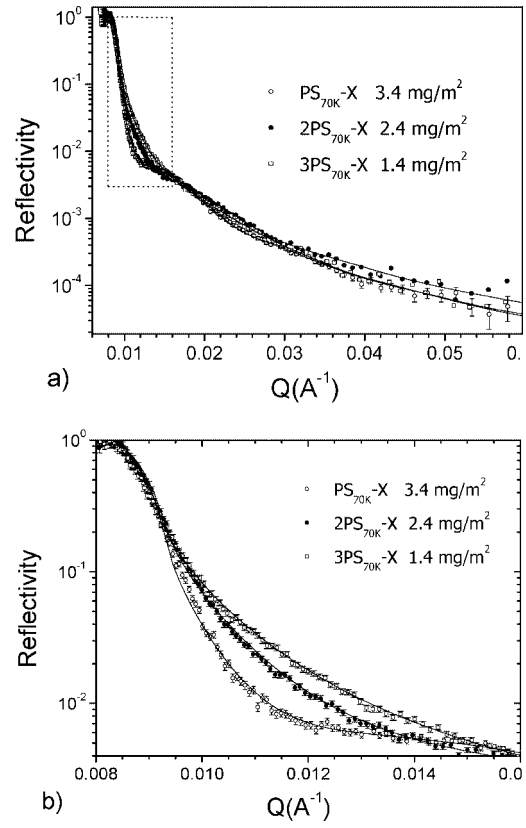

Figure 2. (a) Neutron reflectivity measurements of $f$$PS_{70K}$-X (with f = 1 (○), f = 2 (●), f = 3 (□) end-adsorbed on quartz from d-toluene The continuous lines are least-squares fits based on volume fraction profiles as shown in Figure 3 with parameters given in Table 2. Experimental errors are shown only for one set of data for reasons of clarity. (b) Region of small wavevectors (dotted box in (a)) is magnified.

that the chains attach to the substrate via the zwitterionic group "X" and that the adsorption process occurs over a period of many hours.[10,28,29] Adsorption was allowed to take place for at least 50 h, and measurements were carried out periodically during this time. After the first 6 h of adsorption, subsequent measurements showed no observable change in the volume fraction profiles of the adsorbed polymers. The adsorbance plateau is reached at very low values of bulk solution concentration. The final adsorbance attained remains unchanged when the bulk concentration is in the range 5×10^{-2}−1 mg/mL.

The possibility of brush replacement was studied on a preformed $3PS_{70K}$-X brush by adding PS_{70K}-X copolymer to the solution already containing $3PS_{70K}$-X. Note that in this two-component solution both copolymers have an equal concentration of 0.1 mg/mL.

The polymer volume fraction profiles used to fit the neutron reflectivity data (Figures 2 and 4) were parabola-like (Figures 3 and 5) (i.e., of the form, $a - bz^n$ where the exponent n was allowed to vary) with an approximately Gaussian tail. This functional form allows the profile to become parabolic for n = 2 and linear for n = 1, while for n < 1 it becomes concave upward. The Simplex method was used as a fitting routine to minimize the sum of the weighted squared differences between the experimental points and the fitted reflectivity curves with respect to the fitting parameters. In agreement with earlier studies[8,26,30] of brushes consisting of linear PS chains in good solvent, values very close to n = 2 were found for PS_{70K}-X. It should be stressed that the data could not be fitted well using other functional forms (e.g., linear, exponential, etc.) for the volume fraction profile.

Simulation Methodology

In the computational part of this study, our goal was to perform coarse-grained Monte Carlo simulations in order to gain

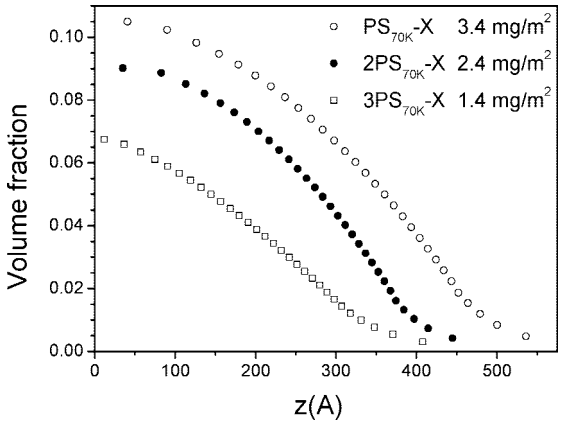

Figure 3. Best-fit volume fraction profiles of the form $a - bz^n$, as discussed in the text, with small Gaussian tails for fPS$_{70K}$-X with $f = 1$ (○), $f = 2$ (●), and $f = 3$ (□) (fitting parameters are given in Table 2).

insight into the kinetics and particularly the equilibrium structure of brushes formed by the self-assembly of star polymers from dilute solutions onto planar substrates. We focused on understanding the equilibrium conformation of adsorbed brushes as a function of the number of arms ($f = 1$, 2, 3) of the star polymers. Furthermore, we studied the replacement effect of three-armed ($f = 3$) grafted chains by the introduction of a linear ($f = 1$) polymer in the bulk solution.

We have adopted a lattice bond fluctuation Monte Carlo (BFMC) technique that has been originally proposed by Carmesin and Kremer[31] and has been used for the study of structure and dynamics of end-grafted brushes.[32,33] This model has also been used for the study of adsorption from bulk solutions of single[34] and double-tethered (i.e., telechelic) chains.[35] The BFMC technique possesses the typical computational advantages of lattice MC methods while the use of fluctuating bond lengths and the many choices of angles between adjoining bond vectors permit the simulation of branched chain structures[36,37] without any ergodicity problems.

Briefly, in the BFMC model each monomer occupies a cube of eight lattice sites on a cubic lattice. Each Monte Carlo step involves a random local displacement in one randomly selected direction of a random monomer and the implementation of the excluded volume and bond length criterion. The allowed bond vectors connecting two neighboring monomers may only have a length equal to 2,$\sqrt{5}$, $\sqrt{6}$, 3, or $\sqrt{10}$.[38] The choice of this set of bond vectors ensures that two bonds cannot cross each other.

To model the adsorption of the end or center-functionalized chains onto the grafting wall (xy plane), we allow an energy $\Delta = 8k_BT$ to be gained when the end (for $f = 1$) or center (for $f = 2$, 3) monomer is situated on the surface since it is known that the sticking energy of the zwitterionic anchoring group is ca. $8k_BT$.[8,10] So a move involving the departure of the end (for $f = 1$) or center (for $f = 2$, 3) monomer from the grafting wall is only accepted if the Boltzmann factor $e^{-\Delta/k_BT}$ is greater than a uniformly distributed random number between 0 and 1.

Polymer chains each consisting of f arms of N monomers (Figure 6) are placed in a $L \times L \times D$ box. L was equal to 100 while D was set equal to 400. We choose a large value for D because we want to keep the bulk solution concentration relatively constant during the adsorption procedure so that the final number of adsorbed chains is not largely affected by chain depletion. The monomer concentration inside the box was $\phi_{bulk} = 0.025$ (dilute regime) in all simulations. The number of monomers of each arm N was equal to 10, 15, 20, 25, or 30. Much longer chains are impractical to handle due to the long computing times required. Periodic boundary conditions are

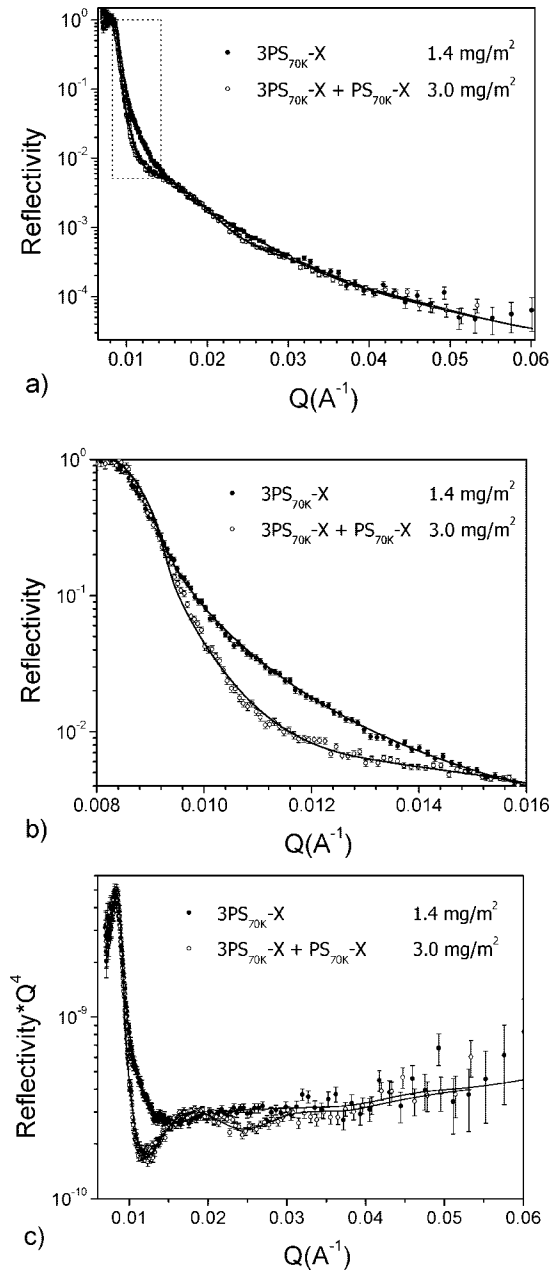

Figure 4. (a) Neutron reflectivity measurements of brushes adsorbed onto quartz from 3PS$_{70K}$-X (●) solution and 3PS$_{70K}$-X + PS$_{70K}$-X (○) mixed solution, both with d-toluene as solvent, are plotted as reflectivity vs Q. The continuous lines are least-squares fits based on parabolic volume fraction profiles with parameters given in the text. (b) Region of small wavevectors (dotted box in (a)) is magnified. (c) Neutron reflectivity measurements shown in (a) are plotted as RQ^4 vs Q. The continuous lines are least-squares fits. The slight rise in the data points seen at higher Q values is due to a thin hydrated surface layer of low scattering length density, typically present when undried d-toluene is used.

imposed in the x,y directions while monomers cannot cross the two planes situated at $z = 1$and $z = D$. Time t is measured in units of MC steps per monomer (MCS).

Beginning with random placement of the chains inside the simulation box, equilibration of the system was carried out by performing about 10^7 MCS. During the equilibration procedure the functional group energy is set equal to zero. Then the functional group energy is "turned on", and about 10^8 MCS are performed in order to simulate the adsorption process. Each simulation run provides two sets of data corresponding to the two adsorbing substrates at $z = 1$ and $z = D$. During adsorption,

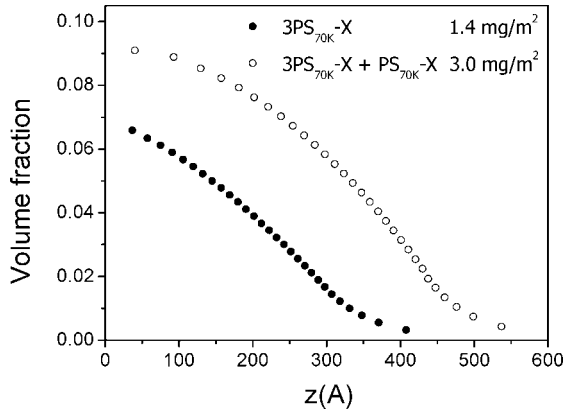

Figure 5. Best-fit volume fraction profiles with small Gaussian tails for $3PS_{70K}$-X (●) and $3PS_{70K}$-X + PS_{70K}-X (○) polymer solutions (fitting parameters are given in the text).

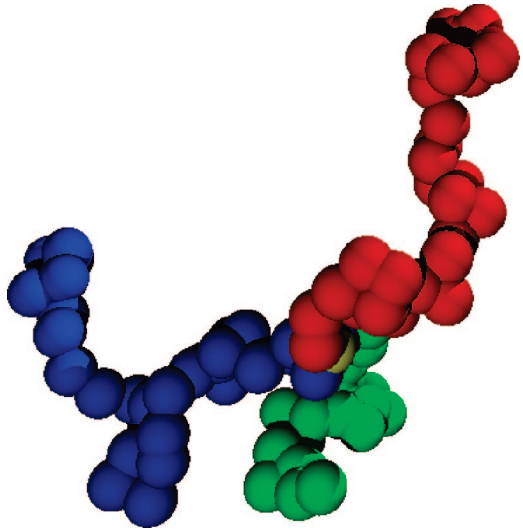

Figure 6. Simulation snapshot where a 3-armed chain (30 monomers per arm) in solution is illustrated. Every arm is denoted with a different color.

Table 2. Neutron Reflectivity Results

no. of arms	adsorbance Γ (mg/m^2)	brush height L_0 (Å)	exponent n	interanchor distance s (Å)	reduced coverage σ^*
1	3.4	490	1.95	58	7.4
2	2.4	400	1.78	98	6.0
3	1.4	354	1.40	158	3.0

several interesting quantities are measured and stored such as the number of adsorbed chains per unit area σ, the number of adsorbed monomers per unit area Γ, the monomer volume fraction profile, and the volume fraction profile of free chain ends.

To demonstrate the replacement of branched chains by linear ones, we consider a system consisting of both three-armed and linear chains. As above, the number of monomers N of the linear chain is equal to the number of monomers of each arm. The concentration of linear and three-armed chains inside the simulation box is $\phi_{3arms} = \phi_{linear} = 0.02$ so that the total monomer concentration is $\phi_{bulk} = 0.04$.

We begin the simulation by performing about 10^7 MCS for system equilibration. At this stage the interaction energy of the functionalized monomer groups is set to zero. Then the interaction energy of the branched chains is set equal to $8k_BT$, and the adsorption, of three-armed chains is recorded for 10^8 MCS. At this point where the three-armed brush formation has fully advanced, the interaction energy of linear chains is also "turned on" and the simulation is carried on, monitoring the adsorbed amount of both chain types for 10^8 MCS.

Results and Discussion

a. Equilibrium Properties. A summary of the experimentally determined equilibrium properties of the centrally tethered star-polymer brushes we studied is presented in Table 2. As can be seen, the data clearly suggest an increase of the mean distance between the zwitterion anchor points upon increasing the number of arms of the star polymer. So the presence of multiple chain arms directly affects the tendency of the copolymers to adsorb on the surface.

This trend is reflected on the final adsorbed amounts measured by NR. We observe a decrease of the total adsorbed amount for increasing number of chain arms. The detailed volume fraction profiles of the brush layers that were obtained from NR measurements (Figure 3) reveal that linear PS_{70K}-X has the highest adsorbance of 3.4 mg/m^2 as well as the most extended brush chain into solution, the adsorbed layer thickness (or brush height) being ca. 500 Å, while the exponent n of the volume fraction profile is nearly equal to 2, i.e., the profile is essentially parabolic. The interanchor spacing s is calculated to be ca. 58 Å, and the reduced coverage[39] $\sigma^* = \pi R_g^2/s^2 = 7.4$. The adsorbance of $2PS_{70K}$-X is 2.4 mg/m^2, and the brush height is lower, relative to the PS_{70K}-X, i.e. ~400 Å, while the exponent n is less than 2. The interanchor spacing s is calculated to be ca. 98 Å, and $\sigma^* = 6.0$.

Finally, the volume fraction profile of $3PS_{70K}$-X has the lowest adsorbance of 1.4 mg/m^2 and the least extended chains into solution since the brush height is ca. 350 Å, while the exponent n is 1.4. The interanchor spacing s is calculated to be 158 Å and $\sigma^* = 3.0$. This low value of the exponent n together with the value of the reduced coverage is indicative of departure from the pure brush regime that predicts a parabolic profile (i.e., $n = 2$) for $\sigma^* \gg 2$. It seems that this deviation of the profile exponent is not related to the conformational restrictions that are imposed by the three-armed star structure, a fact that is also supported by fixed surface density BFMC simulations (results not shown) since for relatively dense linear and branched chain brushes of the same grafting density, no significant differences in the monomer volume fraction profile are observed.

In order to test data reproducibility, two sets of NR measurements were obtained during two different experiments at the EROS spectrometer. The differences in brush profiles between these two experimental sets, both for the adsorbance and for the height of each brush, were found to be within the experimental error. Comparable adsorbance values for linear end-adsorbed polystyrenes have been obtained by surface plasmon resonance methods.[42]

To our knowledge there exists no detailed theoretical treatment of brush systems as those studied in the present work. The scaling theory of Alexander[5] and de Gennes[6] applies to brush systems formed by linear chains. This theory predicts that the layer thickness (or height) L_0 of a semidilute polymer brush in a good solvent is given by

$$L_0 \cong a^{5/3} N s^{-2/3} \tag{1}$$

where N is the polymerization index, s is the mean distance between anchor points, and a is the monomer size. The higher polymer segment concentration due to the attachment of the chains to the surface increases the overall osmotic repulsion, causing them to stretch away from the grafting surface. This tendency is opposed by an elastic restoring force of entropic origin. The balance between these antagonistic trends is what determines the brush height L_0. In end-adsorbed (as opposed to chemically grafted) brushes s is not fixed but variable and

depends on the sticking energy $\varepsilon k_B T$ per chain. Since the number of "blobs" of size s per chain is L_0/s and each blob contributes osmotic repulsion of order $k_B T$, the total repulsion per chain being counterbalanced by the sticking energy at equilibrium, it follows that

$$(L_0/s)k_B T \cong \varepsilon k_B T \tag{2}$$

or

$$L_0 \cong s\varepsilon \tag{3}$$

When this result is combined with eq 1, we finally obtain

$$L_0 \cong a\varepsilon^{2/5} N^{3/5} \tag{4}$$

The 3/5 exponent with varying N has previously been confirmed experimentally.[8,10] Also in this blob picture of the polymer brush one may calculate that the adsorbed amount scales as $\Gamma \propto \varepsilon^{6/5} N^{-1/5}$. As would be expected for nonlinear end-tethered polymers, the present experimental results (Table 2) do not follow any of these power laws.

We may gain some insight into the behavior of centrally adsorbed star polymers by consideration of the Daoud and Cotton[20] theory for star polymers in good solvent. According to these authors, apart from a central ("core") region where the polymer segment concentration is high, further away from the center the arms of a star are in the semidilute regime and therefore stretched in the radial direction due to excluded volume interactions. As the monomer concentration varies radially, it follows that the blob size ξ must also vary along the radius of the star polymer. They predict that the star polymer size, R, varies as

$$R \cong a f^{1/5} N^{3/5} \tag{5}$$

where f is the number of arms, N is the number of monomers per arm, and a is the monomer size. Consider the case of a three-armed PS polymer attached to a surface via a short PB arm terminating in a zwitterion. It is obvious that this mode of attachment brings the PS arms closer together than they would be if the stars were free in solution, causing the local segment concentration to rise. This implies further stretching of the chains, which however must be counterbalanced by the sticking energy of the zwitterion. Clearly, this also imposes limits on the proximity of neighboring stars. If the total osmotic repulsion per star polymer were to exceed the sticking energy of the zwitterion, the polymers would detach. Thus, one may expect a three-armed star attached via a zwitterion to exhibit a lower grafting density (or adsorbance) than a single chain attached via the same zwitterion, a fact that is confirmed by the significantly lower measured adsorbed amount and higher interanchor distance of the former in comparison to that of the latter (see Table 2).

We may proceed further by calculating the mean number of blobs per single star polymer in solution. The mean monomer concentration in the star polymer is

$$c = fN/R^3 \tag{6}$$

In the semidilute regime this implies a mean blob size of $\xi \cong a^{-5/4} c^{-3/4}$. Combining this with eqs 5 and 6, we obtain

$$\xi \cong a f^{-3/10} N^{3/5} \quad (\text{or } \xi \sim f^{-3/10} \text{ for fixed } N) \tag{7}$$

One may then simply argue that the average number of blobs per star is $\bar{n}_0 \cong R^3/\xi^3$. It follows from eqs 5 and 7 that for fixed N

$$\bar{n}_0 \cong f^{3/2} \tag{8}$$

Of course this consideration concerns star polymers in solution. The question arises, therefore, what happens when such a star polymer adsorbs? As can be seen in Figure 7a, the star polymer adsorbs through its core onto the surface. We can assume that all the star arms are now constricted into a hemispherical area,[22] while previously they were occupying a whole spherical volume (Figure 7a). We can thus consider an imaginary mirror image just under the surface completing the sphere. In this sense, we now have a star with exactly double the number of arms $2f$. The average number of blobs per star polymer is now $\bar{n}_b \cong (2f)^{3/2}$. The change in the number of blobs per star before and after adsorption is $\Delta\bar{n}_b = \bar{n}_b - \bar{n}_0 = (2f)^{3/2}/2 - f^{3/2} \cong 0.4 f^{3/2}$.

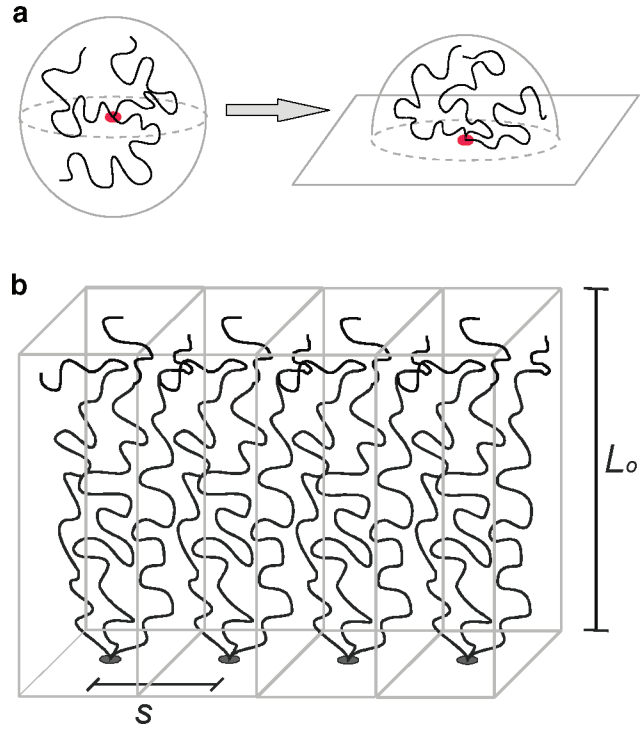

Figure 7. (a) A star in solution (left) and a centrally adsorbed star on a surface, confined into a hemispherical area (right). Note that the "effective" number of arms is doubled when the star is centrally adsorbed onto the substrate. (b) Schematic illustration of a brush formed by center tethered 3-armed star polymers. Every star polymer occupies a rectangular parallelepiped of edge s and height L_0.

The interaction energy $\Delta\bar{n}_b k_B T$ of an adsorbed star polymer must be compensated by the sticking energy $\varepsilon k_B T$. Assuming that the sticking energy is approximately $7-8 k_B T$[10] and setting $\Delta\bar{n}_b k_B T = \varepsilon k_B T$, we conclude that adsorption is no longer possible for $f \geq 6.5$. According to this result, we can assume that a star with more than six arms will hardly adsorb onto the surface.

Returning to the centrally adsorbed star polymer layer (Figure 7b), we may now attempt to calculate the ratio L_0/s, which is a measure of the degree of chain extension in the center-adsorbed brush. We proceed by calculating the mean number of blobs, $\bar{n}_b$, per adsorbed star polymer in the brush

$$\bar{n}_b \cong L_0 s^2/\xi^3 \tag{9}$$

where $L_0 s^2$ is the volume occupied by a center-adsorbed star and ξ is the mean blob size. We may also express L_0 in terms of n_b and ξ, i.e.

$$L_0 \cong (\bar{n}_b/f)\xi \tag{10}$$

where $\bar{n}_b/f$ is the mean number of blobs per arm. Combining eqs 9 and 10, we obtain

$$L_0/s \cong \bar{n}_b f^{-3/2} \tag{11}$$

We may next relate $\bar{n}_b$ to the sticking energy, $\varepsilon k_B T$, of the anchor group. We begin by noting that the monomers of a star

Table 3. Scaling Theory, Experimental, and BFMC Simulation Results Concerning the Ratio between Brush Height L_0 and Interanchor Distance s for Different Numbers of Arms

no. of arms	L_0/s scaling theory[a]	$\overline{L_0/s}$ NR experiments	$\overline{L_0/s}$ BFMC simulations
1	9.0	8.4	8.1
2	3.7	4.1	3.7
3	2.8	2.2	2.4

[a] Based on eq 13 (see text) with $\varepsilon = 8$.

polymer in solution are in the semidilute regime with an average number of blobs $\bar{n}_0 \cong f^{3/2}$ as noted before. Since the monomer concentration in the adsorbed layer is higher, due to the close proximity of neighboring star molecules on the substrate, it follows that the blobs must be smaller and more numerous relative to the free star polymer in solution. This extra number of blobs, $\Delta\bar{n}_b$, formed by virtue of the fact that a previously free star polymer is now participating in the adsorbed layer, costs additional repulsive energy (of order k_BT per blob), which must be compensated by the sticking energy if the star molecule is to remain adsorbed. Thus, at equilibrium

$$\Delta\bar{n}_b k_B T = \varepsilon k_B T \tag{12}$$

where $\Delta\bar{n}_b = \bar{n}_b - \bar{n}_0$. Combining this result with eqs 11 and 8, we obtain

$$L_0/s \cong \varepsilon f^{-3/2} + 1 \tag{13}$$

In Table 3, we see that the ratio L_0/s that is calculated from eq 13 for $f = 1, 2, 3$ is in good agreement with the results from the NR experiments despite the usual limitations of the simple scaling approach presented. These scaling arguments, although unsophisticated, appear to adequately account for the progressively reduced degree of chain stretching and adsorbed amount as a function of the number of arms. It is clear that as f increases, so does the osmotic repulsion within the adsorbed layer until the sticking energy of the zwitterionic anchor group is no longer sufficient to maintain the star polymers tethered to the surface.

It is of interest to compare the behavior of our star polymer brush system to starlike brushes formed by ABA triblock copolymers where tethering is accomplished via the B-block. Dhoot et al.[12] have studied PS−PVP−PS triblocks of this type. In this case, there is considerable space between the two PS chains (i.e., there is an absence of the internal topological constraints inherent in our star polymers), and the system behaves just like a diblock copolymer-based brush that would be formed by cutting the triblock chains in the middle.[12]

The BFMC simulation runs associated with the adsorption of linear, 2-armed, and 3-armed end- or center-functionalized chains produced results that were qualitatively similar to the experimental ones. As the number of arms increases, both the final adsorbed amount and the overall adsorption rate get lower (Figure 8). The latter is primarily due to the higher number of monomers per chain that lowers chain diffusion while the existence of multiple arms hinders the functional core's accessibility to the surface. Large chain rearrangements have to take place in order for the centrally located anchor group to reach and graft on the surface.

For the range of arm lengths studied $N = 10-30$, the relative total adsorbed amount ratios between linear and branched chains (Table 4) are almost independent of N and are directly comparable to the experimental ones. We have found that $\Gamma_{2arms}/\Gamma_{linear} \approx 0.64$ and $\Gamma_{3arms}/\Gamma_{linear} \approx 0.46$, giving a power law $\Gamma \propto f^{-0.70\pm0.04}$. The experimentally measured values for these two ratios are 0.68 and 0.42, respectively, suggesting the power law $\Gamma \propto f^{-0.75\pm0.10}$(Figure 9). Similarly in the case of the interanchor distance ratios NR gave $s_{2arms}/s_{linear} \approx 1.70$ and $s_{3arms}/s_{linear} \approx 2.70$ while BFMC gave $s_{2arms}/s_{linear} \approx 1.76$ and $s_{3arms}/s_{linear} \approx 2.66$.

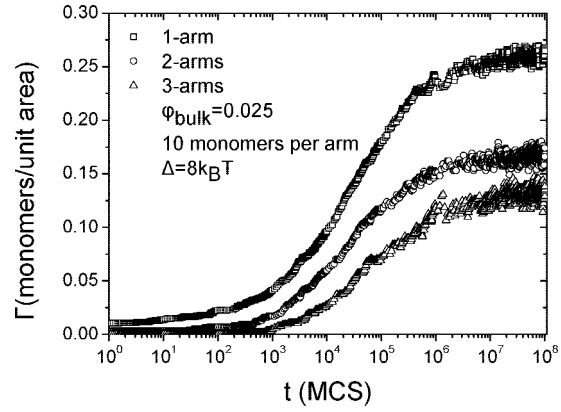

Figure 8. Long-time BFMC adsorption kinetics of a linear, two-arm, and three-arm chain of 10 monomers per arm. Bulk solution concentration is set equal to 0.025.

Table 4. BFMC Simulation Results (Adsorbance Γ and Interanchor Distance s Ratios) for the Adsorption of Linear and Star Polymers of Different Numbers of Monomers on the Grafting Surface

monomers per arm	$\Gamma_{2arms}/\Gamma_{linear}$	$\Gamma_{3arms}/\Gamma_{linear}$	s_{2arms}/s_{linear}	s_{3arms}/s_{linear}
10	0.63	0.47	1.77	2.52
15	0.67	0.46	1.80	2.66
20	0.63	0.45	1.78	2.57
25	0.62	0.43	1.73	2.68
30	0.64	0.48	1.73	2.89

We have mentioned above that scaling arguments (eq 13) concerning the ratio L_0/s are in very good agreement with the data from NR. This agreement is also confirmed by our BFMC simulations. The L_0/s values calculated by BFMC for $f = 1, 2, 3$ compare favorably both with the scaling theory and experiment (Table 3).

Finally, the volume fraction profiles obtained by the BFMC simulations (Figure 10), except for the model-inherent depletion layer near the grafting plane, show no appreciable change on the form of the volume fraction profile due to the special architecture of star polymers while the trend concerning the layer thickness is the same as in our experiments.

This agreement between simulation and experiment suggests that the BFMC model we have adopted, despite the relatively small number of monomers per arm, succeeds in capturing the main features of the behavior of star polymers (at least with 2 and 3 arms) that attach to a surface via a centrally located anchor

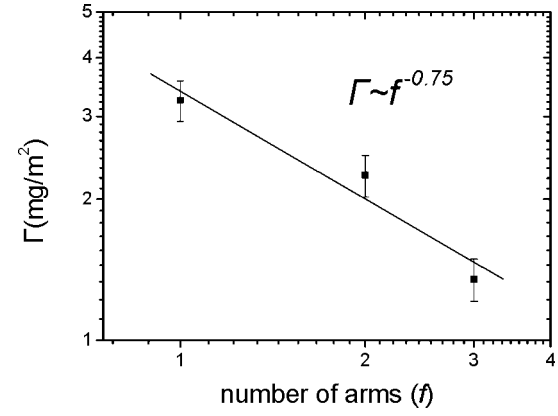

Figure 9. Experimentally measured (averaged values from two different NR data sets) adsorbed amounts for the three different copolymers. A linear fit to the data suggests the power law $\Gamma \sim f^{-0.75\pm0.10}$.

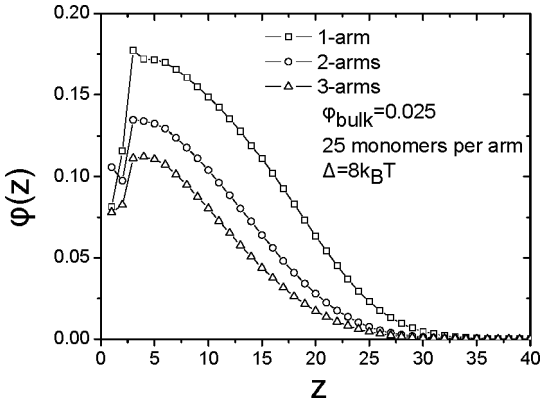

Figure 10. Monomer volume fraction profiles after 10^8 MCS for three different chain solutions ($f = 1$, 2, 3 and $N = 25$) of the same concentration $\phi_{bulk} = 0.025$.

group. On this basis, we extended our simulations to the case of mixed linear/star polymer solutions. We present these results together with the experimental ones in the next section.

b. Brush Replacement Experiments. We studied the influence of addition of PS_{70K}-X copolymer on a surface already covered by a $3PS_{70K}$-X copolymer brush. Neutron reflectivity measurements show that the adsorbed $3PS_{70K}$-X brush on the interface was at least partially replaced by end-grafted PS_{70K}-X chains within a few hours. Analysis of the reflectivity data (Figure 4) indicates that the adsorbance has increased from 1.4 to 3.0 mg/m^2 and does not measurably change any further after 12 h. As can be seen from the volume fraction profiles (Figure 5), the brush height has also increased from 350 to 480 Å while the form of the profile is again nearly parabolic (i.e., $n \simeq 2$) recovering from the initial value $n = 1.40$. These findings indicate that considerable replacement of branched chains takes place.

This overall effect of $3PS_{70K}$-X brush replacement by a PS_{70K}-X brush may be easily attributed to the higher entropic penalty of chain stretching related to branched chain adsorption on the surface. For the same anchor group (and hence the same sticking energy) end-adsorbed *linear* chains are able to pack closer before significant stretching occurs in comparison to the corresponding centrally tethered starlike polymers.

Simulations where after the formation of a 3-armed brush, linear chains are "allowed" to adsorb on the surface, clearly illustrate the considerable replacement effect that takes place. In Figure 11, we present the volume fraction profile of both chain types before and after linear chain adsorption while in Figure 12 the kinetics of replacement are illustrated. The system parameters were $\phi_{3arm} = \phi_{linear} = 0.02$, $\Delta = 8k_BT$.

These results are qualitatively similar to our experimental data from neutron reflectivity measurements. The total adsorbed amount increases, and the brush height is enhanced (Figure 11). We have observed that the relative adsorbed amounts before and after the adsorption of linear chains is strongly dependent on the number of monomers per chain. As the number of monomers increases, there is a lowering of this relative adsorption ratio.

At equilibrium the final brush is comprised of both linear and 3-armed chains. The relative amount of grafted 3-armed and linear polymers in the mixed brush and the rate of replacement depend on their chain/arm lengths and bulk solution concentration. In all simulations the final population of linear chains inside the brush is at least 10 times larger than that of 3-armed chains. Indications of this considerable replacement effect are also evident in the present NR results; however, use of selectively labeled chains would be more appropriate for a more detailed study.

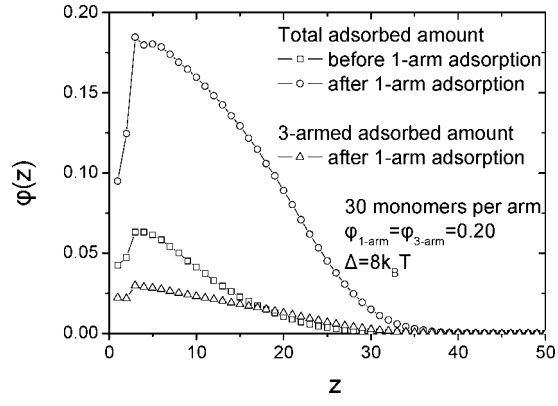

Figure 11. Brush replacement BFMC simulation. A 3-armed star brush is allowed to form first (squares), and subsequently linear chains are allowed to adsorb on the substrate (circles). The total adsorbed amount is shown before and after the onset of linear chain adsorption. Note the enhanced total adsorbed amount and brush height. Also the partial adsorbed amount of 3-armed chains (triangles) after the incorporation of linear chains is shown.

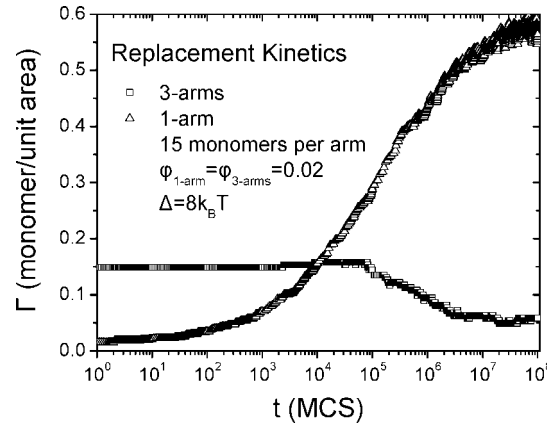

Figure 12. Typical brush replacement kinetics as determined by BFMC simulations.

It should be mentioned that chain replacement effects as those mentioned above are of considerable interest because they may serve as model systems for the interpretation of phenomena that are related to biomacromolecular adsorption from multicomponent solutions. For example, the great diversity of proteins that appear in human body fluids gives rise to complicated surface adsorption behavior of the various species that is dependent on their size, structure, mobility, concentration, relative affinity, etc.

Conclusions

The combined NR and BFMC study of centrally adsorbed starlike polymers on solid surfaces revealed interesting features related to their special chain architecture. The presence of multiple arms in a single star-shaped macromolecule results in a significant decrease of the adsorbance and a corresponding increase of the mean interanchor spacing due to repulsive interactions between neighboring chain arms. The simulation of star polymer adsorption by the BFMC method was found to adequately reproduce the main features of the systems under study. Both the effect of increasing the number of arms on adsorption and the replacement of a centrally adsorbed 3-armed star by linear chains are well described by the BFMC simulation. Furthermore, our scaling analysis suggests that scaling arguments, although simple, can be of value toward aiding our understanding of centrally tethered star polymer behavior. Further experiments involving higher chain branching[43] and

variable molecular weights together with theoretical and computer simulation studies may generalize the present results and elucidate the mechanism of adsorption of centrally adsorbed star polymers in greater detail.

References and Notes

(1) Zhao, B.; Brittain, W. J. *Prog. Polym. Sci.* **2000**, *25*, 677–710.
(2) Tirrel, M.; Levicky, R. *Curr. Opin. Solid State Mater. Sci.* **1997**, *2*, 668–672.
(3) Currie, E. P. K.; Norde, W.; Cohen Stuart, M. A. *Adv. Colloid Interface Sci.* **2003**, *100*, 205–265.
(4) Klein, J. *Annu. Rev. Mater. Sci.* **1996**, *26*, 581–612.
(5) Alexander, S. *J. Phys. (Paris)* **1977**, *38*, 983–986.
(6) De Gennes, P. G. *Adv. Colloid Interface Sci.* **1987**, *27*, 189–209.
(7) Hadziioannou, G.; Patel, S.; Granick, S.; Tirrell, M. *J. Am. Chem. Soc.* **1986**, *108*, 2869–2876.
(8) Field, J. B.; Toprakcioglu, C.; Ball, R. C.; Stanley, H. B.; Dai, L.; Barford, W.; Penfold, J.; Smith, G.; Hamilton, W. *Macromolecules* **1992**, *25*, 434–439.
(9) Sakellariou, G.; Pispas, S.; Hadjichristidis, N. *Macromol. Chem. Phys.* **2003**, *204*, 146–154.
(10) Taunton, H. J.; Toprakcioglu, C.; Fetters, L. J.; Klein, J. *Macromolecules* **1990**, *23*, 571–580.
(11) Watanabe, H.; Tirrel, M. *Macromolecules* **1993**, *26*, 6455–6466.
(12) Dhoot, S.; Watanabe, H.; Tirrell, M. *Colloids Surf., A* **1994**, *86*, 47–60.
(13) Hadjichristidis, N.; Pispas, S.; Pitsikalis, M. *Prog. Polym. Sci.* **1999**, *24*, 875–915.
(14) Irvine, D. J.; Mayes, A. M.; Griffith-Cima, L. *Macromolecules* **1996**, *29*, 6037–6043.
(15) Carignano, M. A.; Szleifer, I. *Macromolecules* **1994**, *27*, 702–710.
(16) Sikorski, A.; Romiszowski, P. *Macromol. Symp.* **2004**, *217*, 273–279.
(17) Romiszowski, P.; Sikorski, A. J. *Chem. Inf. Comput. Sci.* **2004**, *44*, 393–398.
(18) Likos, C. N. *Phys. Rep.* **2001**, *348*, 267–439.
(19) Rissanou, A. N.; Vlassopoulos, D.; Bitsanis, I. A. *Phys. Rev. E* **2005**, *71*, 011402.
(20) Daoud, M.; Cotton, J. P. *J. Phys. (Paris)* **1982**, *43*, 531–538.
(21) Ohno, K.; Binder, K. *J. Chem. Phys.* **1991**, *95*, 5444–5458.
(22) Jusufi, A.; Dzubeilla, J.; Likos, C. N.; von Ferber, C.; Lowen, H. *J. Phys: Condens. Matter* **2001**, *13*, 6177–6194.
(23) Shida, K.; Ohno, K.; Kimura, M.; Kawazoe, Y. *J. Chem. Phys.* **1996**, *105*, 8929–8936.
(24) Battaglin, G.; Menelle, A.; Montecchi, M.; Nichelatti, E.; Polato, P. *Glass Technol.* **2002**, *43*, 203–208.
(25) Russell, T. P. *Mater. Sci. Rep.* **1990**, *5*, 171–271.
(26) Karim, A.; Satija, S. K.; Douglas, J. F.; Ankner, J. F.; Fetters, L. J. *Phys. Rev. Lett.* **1994**, *73*, 3407–3410.
(27) Baker, S. M.; Smith, G. S.; Anastassopoulos, D. L.; Toprakcioglu, C.; Vradis, A. A.; Bucknall, D. G. *Macromolecules* **2000**, *33*, 1120–1122.
(28) Dunlop, I. E.; Briscoe, W. H.; Titmuss, S.; Sakellariou, G.; Hadjichristidis, N.; Klein, J. *Macromol. Chem. Phys.* **2004**, *205*, 2443–2450.
(29) Dorgan, J. R.; Stamm, M.; Toprakcioglu, C.; Jerome, R.; Fetters, L. J. *Macromolecules* **1993**, *26*, 5321–5330.
(30) Anastassopoulos, D. L.; Spiliopoulos, N.; Vradis, A. A.; Toprakcioglu, C.; Baker, S. M.; Menelle, A. *Macromolecules* **2006**, *39*, 8901–8904.
(31) Carmesin, I.; Kremer, M. *Macromolecules* **1988**, *21*, 2819–2823.
(32) Lai, P.-Y.; Binder, K. *J. Chem. Phys.* **1991**, *95*, 9288–9295.
(33) Lai, P.-Y.; Binder, K. *J. Chem. Phys.* **1992**, *97*, 586–595.
(34) Lai, P.-Y. *J. Chem. Phys.* **1993**, *98*, 669–673.
(35) Smith, G. D.; Zhang, Y.; Yin, F.; Bedrov, D.; Dadmun, M. D.; Huang, Z. *Langmuir* **2006**, *22*, 664–675.
(36) Brown, S.; Szawel, G. *Macromol. Theory. Simul.* **2000**, *9*, 14–19.
(37) Cecca, A.; Freire, J. J. *Macromolecules* **2002**, *35*, 2851–2858.
(38) Deutsch, H. P.; Binder, K. *J. Chem. Phys.* **1991**, *94*, 2294–2304.
(39) A value of the reduced coverage $\sigma^* = 2$ marks the onset of chain overlap, while layers that are characterized by $\sigma^* > 8$ are well within the brush regime. The radius of gyration R_g values needed for the calculation of the reduced coverage are estimated using ref 40 for PS_{70K}-X and $2PS_{70K}$-X and using ref 41 for $3PS_{70K}$-X.
(40) Roovers, J. E.; Toporowski, P. M. *J. Polym. Sci., Part B: Polym. Phys.* **1980**, *18*, 1907–1917.
(41) Khasat, N.; Pennisi, R. W.; Hadjichristidis, N.; Fetters, L. J. *Macromolecules* **1988**, *21*, 1100–1106.
(42) Koutsioubas, A. G.; Spiliopoulos, N.; Anastassopoulos, D. L.; Vradis, A. A.; Toprakcioglu, C.; Priftis, G. D. *J. Polym. Sci., Part B: Polym. Phys.* **2006**, *44*, 1580–1591.
(43) Glynos, E.; Chremos, A.; Petekidis, G.; Camp, P. J.; Koutsos, V. *Macromolecules* **2007**, *40*, 6947–6958.

MA702749Z